Scripta Materialia 145 (2018) 95–98

Contents lists available at ScienceDirect

Scripta Materialia

journal homepage: www.elsevier.com/locate/scriptamat

Regular article

Thickness-dependent stabilization of tetragonal ZrO_2 in oxidized zirconium

Wayne Harlow [a], Andrew C. Lang [a], Brian J. Demaske [b], Simon R. Phillpot [b], Mitra L. Taheri [a,*]

[a] Department of Materials Science and Engineering, Drexel University, Philadelphia, PA 19104, USA
[b] Department of Materials Science and Engineering, University of Florida, Gainesville, FL 32611, USA

ARTICLE INFO

Article history:
Received 14 April 2017
Received in revised form 8 September 2017
Accepted 8 September 2017

Keywords:
Oxidation
Zirconium
Transmission electron microscopy
Precession electron diffraction
Density functional theory

ABSTRACT

Here we describe a study on the effect of transmission electron microscopy sample preparation on the stability of the tetragonal ZrO_2 phase, as determined by precession electron diffraction. It was found that sample thickness, and thus corresponding stress remaining within the sample, can significantly affect the percentage of tetragonal phase ZrO_2 recorded in the oxide layers. The microscopy-based finding is complemented by density functional theory calculations, confirming that there exists a crossover in energy between the two phases that depends on compressive strain. These findings further confirm that the significant portion of tetragonal phase is the result of stress stabilization.

Zirconium-based alloys have long been used for fuel rod cladding material and, as a result, extensive research into the corrosion behavior of these alloys has been previously conducted [1–4]. One long-standing debate has been the quantification of the oxide phases formed during corrosion; studies have found the presence of two distinct oxide phases: tetragonal phase and monoclinic. One particular question revolves around the role of tetragonal phase of the oxide and how the stability and protectiveness of this phase relates to the cyclic oxidation behavior of zirconium alloys. It is well known that over long-term tests, zirconium alloy samples experience oxide cracking, which may be detrimental to oxidation performance [5–7]. The cyclic oxidation behavior seen in these long-term tests has also been attributed to the formation, transformation to monoclinic, and reformation of the tetragonal oxide phase [5,8–10].

These phases have been characterized using a wide variety of characterization techniques, including X-ray diffraction (XRD) [11–13], microbeam synchrotron diffraction [9,13–15], Raman spectroscopy [16], and transmission electron microscopy (TEM) [17–21], and studied with a variety of theoretical methods [10,22]. The relationship between the distribution of each oxide phase in the oxidation of zirconium and its alloys has been a long-standing question in the field, especially since the tetragonal phase of ZrO_2 is not stable at room temperature except under high stress [23]. Several authors have postulated that an oxide phase may account for the cyclic oxidation behavior seen in long-term oxidation experiments, as the stabilization/destabilization of the oxide phases could account for changes in oxidation behavior [1]. Several in-situ X-ray photoelectric spectroscopy (XPS) and synchrotron XRD studies have shown that tetragonal ZrO_2 is the initial oxide layer that forms [14,24]. However, it has also been shown that the tetragonal phase fraction is reduced when oxide relaxation and transformation to monoclinic occurs [25]. This fits well with the theory that the tetragonal phase acts as the protective phase; the reduction of tetragonal phase due to oxide relaxation correlates well with the abrupt increases in corrosion rate seen in long-term studies. Thus, much effort has been devoted to studying this problem and attempting to draw conclusions regarding the effect of the oxide phases on corrosion behavior.

The appearance of the tetragonal phase in the oxide formed on zirconium during oxidation has long been attributed to the stress present in the oxide. When considering how good a protective passive oxide layer is on a metal it is common to use the Pillings-Bedworth ratio, which is 1.56 for this oxide/metal system [16]. This implies that this coating has the potential to be protective, but it also implies that there will be a high compressive stress in the oxide film. Recently, studies by Platt et al. have looked at the stress stabilization of the tetragonal phase via finite element modeling and showed that the transformation from tetragonal ZrO_2 to monoclinic ZrO_2 could indeed be the result of reduction in stress of the oxide [22]. Previously, Garner et al. [19] and Harlow et al. [21] showed that using precession electron diffraction is a reliable method for identifying tetragonal and monoclinic ZrO_2 phases. Other authors have indicated that grain size may also affect the stabilization of the tetragonal phase [10,26]. In this work, we describe a systematic

* Corresponding author.
E-mail address: mtaheri@coe.drexel.edu (M.L. Taheri).

https://doi.org/10.1016/j.scriptamat.2017.09.014
1359-6462/

study of the thickness dependence of tetragonal phase fraction in ZrO_2 using TEM, precession electron diffraction, and density functional theory (DFT), and find that the stress stabilization of the tetragonal phase is confirmed using this methodology. Our findings also provide a foundation for the study of how TEM sample thickness is likely to affect the amount of tetragonal phases observed within an oxidized sample via precession electron diffraction and electron energy loss spectroscopy.

Pure zirconium samples, autoclave oxidized by Motta et al. [27] were used as an idealized system in order to eliminate any effect of alloying elements or impurities on the oxide phase stability. Samples were made from several regions within the oxidized sample so as to limit any localized stress effects from the base metal. In order to test the theory that the sample relaxes and reduces the amount of tetragonal ZrO_2 present changes, a sample was prepared with a series of controlled thicknesses (Fig. 1). Focused Ion Beam (FIB) was used to prepare a "stepped" sample that had multiple thicknesses within it; analyzing several thicknesses within a single specimen eliminates any artifacts, such as local composition variation. Preparation was performed using standard FIB techniques [28] using a FEI DB-235 DualBeam to produce 30 μm-long lamellas. Lift-outs were taken top down into the oxidized pure zirconium material, such that when viewed from the side there was a layered structure of protective platinum from the FIB, oxide, metal. Each sample was thinned such that there were five windows, each five microns wide, with thickness varying from ~300 nm to as thin as possible (~30 nm), with the remaining 5 μm near the edge of the sample being sacrificed to attach the sample to the grid. Multiple samples were constructed in this manner to minimize the possibility of an artifact from either sample preparation or lift out location.

In order to determine the phases present, precession electron diffraction (PED), enabled by the Nanomegas ASTAR™ system, was used to characterize each section of the sample using a JEOL 2100 LaB_6 TEM. Each 5 μm window in the sample was characterized by using PED scans with a spot size of 15 nm and a step size of 2 nm by 2 nm. All scans were taken to include the oxide-metal interface, as this region is expected to have the highest occurrence of tetragonal ZrO_2. It was found that reliable data was only generated over the two thinnest windows, with the reliability of the data being too low to be trustworthy in the three thicker regions once indexed. Relative thickness of the TEM samples was determined using the log-ratio method from electron energy loss spectroscopy (EELS) performed on a JEOL 2100F TEM equipped with a GIF Quantum energy filter.

DFT calculations on ZrO_2 were performed using the VASP software package [29,30]. Projector augmented wave (PAW) pseudopotentials were used to treat the core electrons [31,32], while the $4s^2 4p^6 4d^2 5s^2$ electrons for Zr and $2s^2 2p^4$ electrons for O were treated as valence. The electron density was calculated self-consistently until the change in the total energy is $<10^{-6}$ eV. Integration over the Brillouin zone was performed using the linear tetrahedron method with Blöchl corrections [33]. A plane wave energy cutoff of 800 eV and k-point mesh of $7\times7\times7$ were found to be sufficient to converge the total energy to within 1 meV/atom. Ionic and cell relaxations were carried out using the conjugate gradient algorithm until the maximum force component was <0.01 eV/Å and maximum stress component was <0.01 eV/Ω, where Ω is the cell volume. The exchange-correlation functional is treated in the local density approximation (LDA). The choice of the LDA over the more sophisticated generalized gradient approximation (GGA) was motivated by previous first-principles studies on ZrO_2 and HfO_2, which showed that the GGA tends to produce soft phonons [34–36]. Calculated equilibrium lattice parameters for monoclinic and tetragonal phases of ZrO_2 are given in Table 1.

Table 1
Equilibrium lattice parameters for monoclinic and tetragonal phases of ZrO_2. Theoretical results are for T = 0 K, while experimental results are at room temperature.

	a (Å)	b (Å)	c (Å)	β (deg)	Reference
Monoclinic ($P2_1/c$)	5.087	5.191	5.236	99.42	This work (VASP-LDA)
	5.151	5.212	5.317	99.23	Expt. (Ref. [37])
Tetragonal ($P4_2/nmc$)	3.561	–	5.113	–	This work (VASP-LDA)
	3.606	–	5.180	–	Expt. (Ref. [37])

In the thinnest window of all the samples, PED measured the presence of exclusively monoclinic ZrO_2 and the base metal HCP zirconium. As can be seen in Fig. 2, even in regions where the presence of the tetragonal oxide phase is expected, such as the oxide-metal interface, easily visible in Fig. 2 as the intersection of the green monoclinic phase and the red HCP zirconium phase, precession diffraction shows almost no presence of the tetragonal phase.

Moving to thicker windows, the data consistently shows small concentrations of tetragonal ZrO_2, especially at the expected location of the metal-oxide interface, and within the bulk of the oxide, typically near features like cracks. These results imply that there are clear thickness effects on the percentage of tetragonal ZrO_2 present in the sample, and as such, sample preparation will be an important factor in determining the presence or absence of tetragonal ZrO_2. Fig. 3 shows a thicker sample region as compared to Fig. 2, with a much higher occurrence of the tetragonal phase. When PED is combined with EELS to determine the relationship between the percent tetragonal ZrO_2 in the oxide layer and the relative sample thickness, it is clear that tetragonal ZrO_2 percent increases as thickness increases. At some value, a plateau would be expected, giving an accurate representation of the percent tetragonal in the bulk material; however with precession diffraction, the sample thickness exceeds the thickness allowable for reliable data prior seeing a plateau in the data.

As can be seen in Fig. 4, while there is significant scatter in the percentage of tetragonal phase recorded, the overall percentage of tetragonal phase generally increases as sample thickness increases. Sample

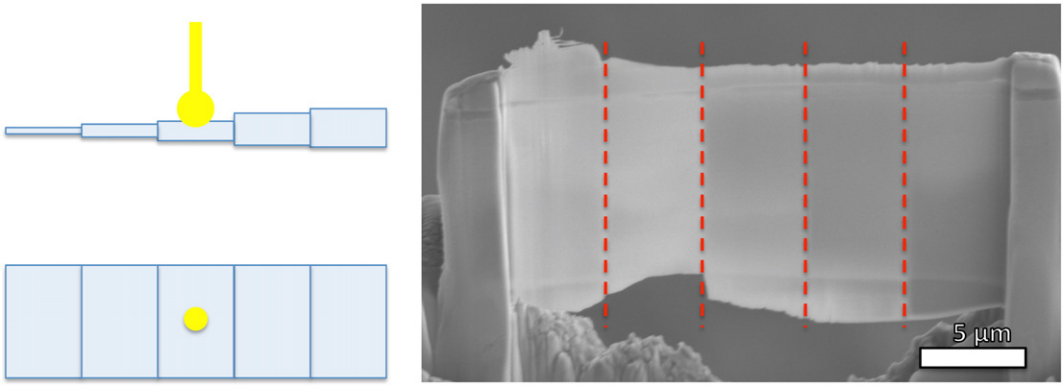

Fig. 1. Schematic on left shows sample appearance in top view and side view with TEM beam direction indicated. On right, an SEM SEI image showing a TEM lamella prepared with multiple thicknesses. The thinnest region of the lamella is on the left with each change in thickness indicated with a dotted line.